Available online at www.sciencedirect.com
SCIENCE DIRECT
Journal of Solid State Chemistry 179 (2006) 2487–2494
JOURNAL OF SOLID STATE CHEMISTRY
www.elsevier.com/locate/jssc

Synthesis, structures and phase transitions in the double perovskites $Sr_{2-x}Ca_xCrNbO_6$

Melina C.L. Cheah[a], Brendan J. Kennedy[a,*], Ray L. Withers[b], Masao Yonemura[c], Takashi Kamiyama[c]

[a]*School of Chemistry, The University of Sydney, Sydney, NSW 2006 Australia*
[b]*Research School of Chemistry, Australian National University, Canberra ACT 2600, Australia*
[c]*Institute of Materials Science, University of Tsukuba, Tsukuba 305-8573, Japan*

Received 2 February 2006; received in revised form 4 April 2006; accepted 5 April 2006
Available online 9 May 2006

Abstract

The synthesis and crystal structures of nine members of the rock-salt ordered double perovskites $Sr_{2-x}Ca_xCrNbO_6$ is presented. The crystal structures of the end members of the series Sr_2CrNbO_6 and Ca_2CrNbO_6 were refined using powder neutron diffraction data and are cubic in $Fm\bar{3}m$ and monoclinic in $P2_1/n$, respectively, in both cases there being considerable anti-site Cr–Nb mixing. Variable temperature and/or composition studies suggest a direct first-order $P2_1/n$ to $Fm\bar{3}m$ transition, a suggestion supported by selected area electron diffraction studies.

Keywords: Perovskite; Phase transition; Chromium niobium oxides

1. Introduction

The remarkable compositional and structural flexibility of the ABO_3 perovskite oxides enables their desirable physical, electrical, magnetic and structural properties to be optimized for specific applications [1]. Where two cations, with significantly different size and/or charge, occupy either the cuboctahedral A-type or octahedral B-type sites these can order, giving rise to exceptional behavior, e.g. colossal magnetoresistance [2,3]. The simplest type of cation ordered perovskites are the $A_2BB'O_6$ double perovskites where the two cations occupying the octahedral sites order in a rock-salt-like arrangement [1,4]. The potential use of such double perovskites in functional materials has prompted immense research efforts in recent years.

Choy et al. [5] recently described the preparation and magnetic properties of the oxides A_2CrNbO_6 (A = Ca, Sr). They reported that both oxides displayed rock-salt-like ordering of the Cr^{III} and Nb^{V} cations, however whereas Sr_2CrNbO_6 was cubic, replacement of the Sr by smaller Ca cations (ionic radii 1.44 vs. 1.34 Å) introduced tilting of the BO_6 octahedra and the resulting structure was monoclinic. Since the ionic radii of Cr^{III} and Nb^{V} are very similar (0.615 vs. 0.64 Å) [6] this ordering is driven primarily by the charge difference, and it is expected that the Nb–O and Cr–O bond distances should be approximately equal. This was apparently observed by Choy et al. [5], although the precision of their structural refinements, that relied on powder X-ray diffraction data collected using non-monochromatic Cu$K\alpha$ radiation, are relatively poor. The average distances in Sr_2CrNbO_6 are Cr–O 1.971(6) and Nb–O 1.966(6) Å and in Ca_2CrNbO_6 Cr–O 1.985 and Nb–O 2.014 Å. Choy et al. suggested that the small differences in bond distances were significant and represented differences in the covalency of the A–O and by extension the B–O bonds.

As part of our on-going studies of phase transitions in perovskite type oxides [7–10] we are interested in the structures of double perovskites where the two B-type cations are of similar size so that the ordering is

*Corresponding author. Fax: +61 2 9351 3329.
E-mail address: kennedyb@chem.usyd.edu.au (B.J. Kennedy).

0022-4596/$ - see front matter
doi:10.1016/j.jssc.2006.04.047

predominantly driven by the charge difference. The aim of the present work was two-fold. Firstly to establish precise and accurate structures and bond distances for Sr_2CrNbO_6 and Ca_2CrNbO_6 using powder neutron diffraction and secondly to study the evolution of the structure as Sr is systematically replaced by Ca in the solid solutions $Sr_{2-x}Ca_xCrNbO_6$.

2. Experimental

Polycrystalline samples of 9 members in the series of solid solutions $Sr_{2-x}Ca_xCrNbO_6$ were prepared by the reaction of the appropriate stoichiometric mixture of $CrNbO_4$, $SrCO_3$, and $CaCO_3$. The reactants were intimately mixed in an agate mortar under acetone, placed in an alumina crucible and heated at 900 °C for 12 h and then at 1200 °C for 1 day with intermediate grinding. $CrNbO_4$ was prepared by reacting Cr_2O_3 and Nb_2O_5 at 1200 °C for 3 days.

The sample purity was established through powder X-ray diffraction measurements using Cu$K\alpha$ radiation on a Shimadzu D-6000 Diffractometer. Synchrotron X-ray powder diffraction data were recorded using the Debye–Scherrer diffractometer on beamline 20B, the Australian National Beamline Facility, at the Photon Factory, Tsukuba Japan [11]. Data were collected in 0.01° steps over the angular range $5° \leqslant 2\theta \leqslant 85°$ using two image plates as detectors. Each image plate is $20 \times 40\,cm^2$ and covers 40° in 2θ. The wavelength of the X-rays used was 0.75049 Å. The samples were held in 0.03 mm dia quartz capillaries that rotated throughout the measurements. Temperature control was achieved using a custom built furnace. Structures were refined using the Rietveld method as implemented in the program RIETICA [12].

Powder neutron diffraction data were recorded, for samples housed in thin walled vanadium cans, on the VEGA diffractometer at KENS [13]. Data collected using the back-scattering bank were used in the structural refinement employing GSAS [14]. Data were obtained for Sr_2CrNbO_6 at both room temperature and at 5 K using a closed cycle cryostat and for Ca_2CrNbO_6 at room temperature.

Electron diffraction patterns (EDPs) from crushed grains of the samples dispersed onto holey carbon coated copper grids were recorded on a Philips EM 430 Transmission Electron Microscope operating at 300 kV.

3. Results and discussion

The use of the rutile-type intermediate phase $CrNbO_4$ in the preparation of the mixed metal perovskites allowed us to prepare highly crystalline single phase samples with precisely controlled Cr:Nb ratios Equally importantly through the use of $CrNbO_4$ it was possible to prepare the oxides in air. Attempts to directly prepare the target perovskites from ACO_3 (A = Ca, Sr), Cr_2O_3 and Nb_2O_5 in air resulted in a mixture of products, although we note that Choy et al. [5] reported the latter approach was successful if the heating was conducted under nitrogen. All the oxides were obtained as olive green powders and the powder X-ray diffraction patterns showed these to be perovskites with superlattice reflections indicative of Cr:Nb ordering being apparent. Quantitative elemental analysis of the various products gave cation ratios within analytical error of the nominal compositions.

In Fig. 1, the powder XRD pattern of Sr_2CrNbO_6 and Ca_2CrNbO_6 profiles obtained by Rietveld refinements are shown. The pattern for Ca_2CrNbO_6 shows clear evidence for a monoclinic structure as reported by Choy et al. [5], whereas the pattern for Sr_2CrNbO_6 is well fitted in the cubic space group $Fm\bar{3}m$, there being no evidence for peak splitting or asymmetry, even at higher angles, indicative of lower symmetry, Fig. 1. The refinements, whilst clearly satisfactory, were relatively insensitive to the oxygen positional parameters and so the structures were refined using TOF neutron powder diffraction data. The neutron diffraction pattern for Sr_2CrNbO_6 recorded at room temperature demonstrated the material to be cubic and cooling to 5 K did not result in any change in symmetry. Attempts to refine the structure in tetragonal ($I4/m$) were unstable unless the O anions were constrained at the equivalent position for $Fm\bar{3}m$. The observed c/a ratio was 1.0003 for the tetragonal fit, and this ratio did not alter on cooling to 5 K. A tetragonal distortion of less than 0.03% is much lower than the instrument resolution. Likewise refinements in $R\bar{3}$ were unstable, and in both cases the refined lattice parameters were indicative of a cubic cell demonstrating these two choices of space group to be

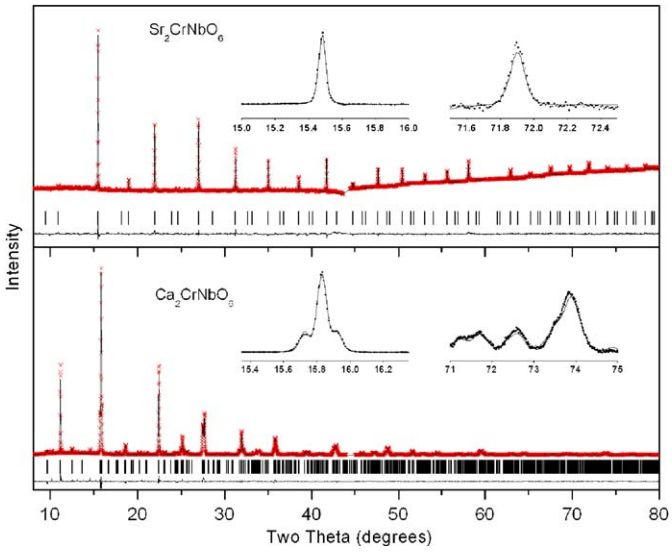

Fig. 1. Observed and calculated synchrotron X-ray diffraction profiles for Sr_2CrNbO_6 and Ca_2CrNbO_6. In each case the bottom curve is the difference profile and the tick marks show the positions of the allowed reflections. The small discontinuity near $2\theta = 45°$ is from the gap between the two image plate detectors. The insets highlight the effects of the change in symmetry. The profiles were fitted with R_p, 2.16 and R_{wp}, 2.86 for Sr_2CrNbO_6 and R_p/R_{wp} of 4.88/6.42% for Ca_2CrNbO_6.

incorrect. The neutron pattern for Ca_2CrNbO_6 at room temperature showed strong superlattice reflections associated with both in-phase and out-of-phase tilting of the MO_6 octahedra and was well fitted in the commonly observed [15] monoclinic space group $P2_1/n$, Fig. 2. For brevity only the refined structural parameters obtained from the neutron diffraction data are listed in Table 1.

For both oxides it was found that the atomic displacement parameters of the B-type cations, as refined using the synchrotron X-ray diffraction data were unusual. For example for Ca_2CrNbO_6 with complete ordering of Cr and Nb had $B_{iso}(Cr) = 0.62$ $B_{iso}(Nb) = 1.55\,Å^3$ R_p, 6.5, R_{wp} 9.1%. This was taken as evidence for a small amount of disorder of these cations over the two possible sites. Introduction of such disorder gave more typical displacement parameters $B_{iso}(Cr) = 1.28(4)$ $B_{iso}(Nb) = 1.25(3)\,Å^3$ and an improvement in the quality of the fit R_p, 5.2, R_{wp} 6.6%. A similar situation occurred for Sr_2CrNbO_6. The neutron diffraction showed similar results and in the final refinements the displacement parameters on the two sites were constrained to be equal. The degree of anti-site disorder observed in this study is somewhat different that that reported by Choy et al. [5], presumably as a result of the different preparative methods used in the two studies. That both preparative methods yield materials with extensive anti-site disorder demonstrates the disposition of Cr and Nb to occupy similar coordination environments, presumably as a consequence of their similar ionic radii.

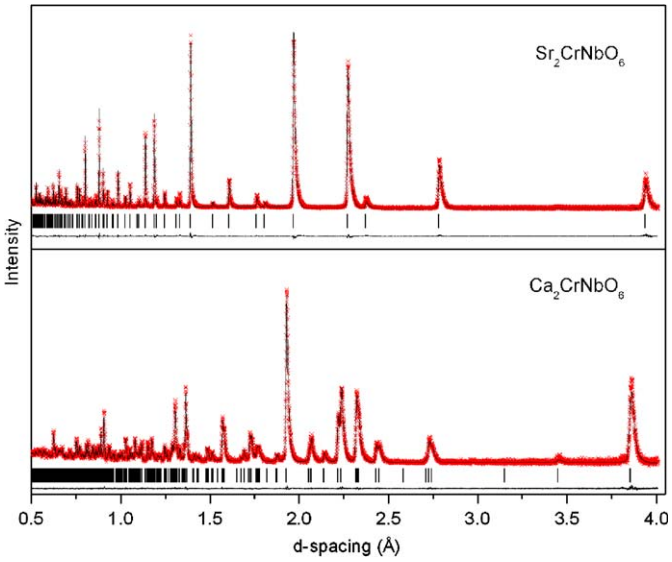

Fig. 2. Observed and calculated time-of-flight neutron diffraction patterns for Sr_2CrNbO_6 and Ca_2CrNbO_6. The format is the same as in Fig. 1. The profiles were fitted with R_p 4.93 and R_{wp} 6.35 for Sr_2CrNbO_6 and R_p/R_{wp} of 4.07/5.59% for Ca_2CrNbO_6.

Table 1
Refined structural parameters for Sr_2CrNbO_6 and Ca_2CrNbO_6 from room temperature time-of-flight neutron diffraction data

Atom	x	y	z	B_{iso} (Å^3)	N
$a = 7.8788(8)$ Å					
Sr	$\frac{1}{4}$	$\frac{1}{4}$	$\frac{1}{4}$	0.68(3)	1
Cr(1)	0	0	0	1.50(1)	0.92(1)
Nb(1)	0	0	0	1.50(1)	0.08(1)
Cr(2)	$\frac{1}{2}$	$\frac{1}{2}$	$\frac{1}{2}$	1.50(1)	0.08(1)
Nb(2)	$\frac{1}{2}$	$\frac{1}{2}$	$\frac{1}{2}$	1.50(1)	0.92(1)
O	0.2503(3)	0	0	0.80(6)	1
$a = 5.4198(2)$, $b = 5.4868(2)$, $c = 7.7060(3)$ Å, $\beta = 89.99(1)^\circ$.					
Ca	−0.0060(7)	0.4622(4)	0.244(2	0.88(5)	1
Cr(1)	0	0	0	0.27(1)	0.76(3)
Nb(1)	0	0	0	0.27(1)	0.24(3)
Cr(2)	0	0	$\frac{1}{2}$	0.27(1)	0.24(3)
Nb(2)	0	0	$\frac{1}{2}$	0.27(1)	0.76(3)
O(1)	0.207(2)	0.287(2)	−0.041(1)	0.21(1)	1
O(2)	0.290(2)	0.796(1)	−0.039(1)	0.66(1)	1
O(3)	0.0766(4)	0.0197(4)	0.251(2)	0.27(5)	1

A detailed discussion of bond-lengths is inappropriate given the extent of the cation disorder, nevertheless it is interesting to examine these. The average Cr–O bond distances in Ca_2CrNbO_6, 1.962(9) Å, is ~0.03 Å shorter than the average Nb–O distance (1.992 Å), this being about the difference in ionic radii, 0.615 vs. 0.64 Å, [6]. The bond valences for the two cations are 3.16 and 4.83 Å. There is no indication from these values for any significant electronic contribution to the bond distances for the BO_6 octahedra. Considering the bond distances in Sr_2CrNbO_6 we find that the Cr–O 1.967(2) Å and Nb–O 1.972(2) Å distances are, within the precision of the measurements identical, that is the Cr–O distance is somewhat longer (or the Nb–O distance shorter) than might be expected based on the tabulated ionic radii. The bond valences for the two cations 3.11 and 5.09 are unexceptional. Whilst it is possible that the observed changes in the relative bond distances reflects changes in the covalency of the Sr–O vs. Ca–O bonds it is more likely that it simply reflects the flexibility of the perovskite structure coupled with the consequence of anti-site disorder.

The cubic perovskite structure is structurally demanding with the bonding requirements of both the A- and B-type cations contributing to its stability. The competing nature of these is often quantified by the tolerance factor given $t = (R_O + R_A)/[\sqrt{2}(R_O + R_B)]$ where R_O is the ionic radii of oxygen, R_A that of the A-type cation and R_B the average radii of the two B-site cations. Deviations from $t = 1$ indicate an unfavorable situation and if $t < 1$, the cation is thought to be too small for the cuboctahedron site and cooperative tilting of the BO_6 octahedra can occur. In the present case, t decreases from 0.990 in the Sr compound to 0.956 in the Ca compound, using the ionic radii for 12-fold coordination on the A-site. It should be noted that with two Ca–O distances of more than 3.3 Å the effective coordination of the Ca site in Ca_2CrNbO_6 is reduced from 12 to 10 whereas in the cubic structure the Sr is 12-coordinate. It is thought that the small changes in the B–O bond distances between $Sr_2CrNbO_6$and Ca_2CrNbO_6 reflect optimization of the various bonding requirements and

should not be taken as evidence for a significant change in the covalency of the individual bonds [5]. As noted above cooling the sample to 5 K does not induce any change in the symmetry of Sr_2CrNbO_6 in keeping with the near optimal A–O and B–O distances.

Having established, using powder neutron diffraction, the correct symmetry for the two oxides A_2CrNbO_6 (A = Ca, Sr) we turn our attention to the solid solutions of the type $Sr_{2-x}Ca_xCrNbO_6$. At the outset we expect at least one intermediate phase between the cubic ($a^0a^0a^0$) and monoclinic ($a^+b^-b^-$) structures due to the successive introduction of tilting of the BO_6 octahedra as the effective size of the A-type cation decreases. Howard et al. [16] recently elaborated the possible space groups for rock-salt ordered double perovskites with various combinations of in-phase and out-of-phase tilting. Their group theory analysis suggests a number of possible intermediate structures. Synchrotron X-ray diffraction patterns were collected for 9 members in the series $Sr_{2-x}Ca_xCrNbO_6$. Visual examination of the patterns showed the three Ca-rich oxides ($x = 2.0$, 1.75, 1.5) to be clearly monoclinic and these structures were all refined in $P2_1/n$.

The diffraction patterns of the remaining oxides indicate these to be metrically cubic. Although the patterns for the three oxides with $x = 1.25$, 1.0, 0.75 could be fitted in the monoclinic structure in $P2_1/n$, in each case we found $a \approx b \approx c$ and $\beta \approx 90.0^\circ$ suggesting the symmetry was higher. The possibility that these were in fact tetragonal was then considered. It should be stressed that in the ideal case the appropriate space group would be established from the splitting of the Bragg reflections and the superlattice extinction conditions. However, in systems where the cell metric appears higher (pseudo-symmetry resulting in the absence of any resolved splitting) it is necessary to use the superlattice reflections alone. A key feature of the present work is the exceptional signal-to-noise afforded by the synchrotron diffractometer that allows for clear identification of the reflections associated with the tilting of the octahedra. These reflections were not observed using the conventional X-ray source.

At this point it is appropriate to review the relationship between the observed superlattice reflections and the tilting of the BO_6 octahedra. In-phase octahedral tilting, associated with an M-point, produces superlattice reflections with *even–odd–odd* indices, and out-of-phase tilting (R-point) produces superlattice reflections with indices *odd–odd–odd*. The simultaneous occurrence of M-point and R-point distortions will produce some X-point reflections, indexing as *even–even–odd*. Such X-point reflections are usually very weak in perovskites, such as $CaMnO_3$ [17] or $CaTiO_3$ [18]; however, in the double perovskites the cation ordering is also associated with an R-point and provided the scattering difference between the two cations is sufficiently strong gives rise to, strong, *odd–odd–odd* reflections. The observation of significant X-ray intensities at the X-points implies cation ordering along with both M-point (+) and R-point (−) octahedral tilting is present. If neutron, rather than X-ray, diffraction is employed then the magnitude of the M- and R-point reflections due to the tilting of the octahedra is expected to be somewhat stronger. It is possible that the difference in scattering lengths of the two B-type cations may be insignificantly small to significantly contribute to the R-point reflections.

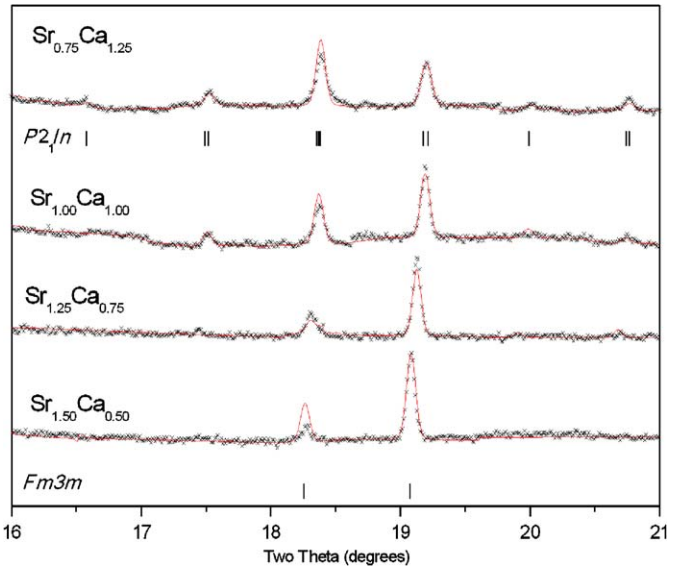

Fig. 3. Portions of the synchrotron X-ray diffraction profiles for $Sr_{2-x}Ca_xCrNbO_6$ showing the growth of intensity of selected superlattice reflections with increasing Ca content. The bottom set of reflection markers show the positions of the reflections allowed in *Fm3m* and the top set show those allowed in $P2_1/n$. Note also the broadening of the (cubic) 222 reflection near $2\theta = 19.0^\circ$ due to the monoclinic distortion. The R-point reflection near $2\theta = 18.3^\circ$ is due to the ordering of the Cr and Nb cations.

Examination of the synchrotron X-ray profiles for $Sr_{0.75}Ca_{1.25}CrNbO_6$ and $Sr_{1.00}Ca_{1.00}CrNbO_6$ near $2\theta = 17.6$ and 20.8° showed, Fig. 3, very weak reflections that could be indexed as 2 1 0 and 2 2 1 on a doubled perovskite cell. From the above discussion the presence of these X point reflections confirms the presence of both in-phase and out-of-phase tilting in these oxides and demonstrates the oxides cannot be tetragonal, in either $I4/m\ a^0a^0c^-$ or $P4/mnc\ a^0a^0c^+$ [16], but rather must be monoclinic in $P2_1/n$ ($a^+b^-b^-$). This choice of space group was further vindicated by successful Rietveld refinements and an example of the refined parameters for (CaSr)CrNNbO$_6$ is given in Table 2. It was not possible to unequivocally establish the tilt pattern from the synchrotron X-ray diffraction pattern for $Sr_{1.25}Ca_{0.75}CrNbO_6$, the diagnostic reflections being extremely weak, having intensity comparable to the noise in the background. The pattern with $x = 1.5$ appears not to have any superlattice reflections associated with tilting of the octahedra.

In order to verify the choice of space group for the four oxides $0.75 \leqslant x \leqslant 1.5$, relevant single domain EDPs were also obtained. These EDPs confirm that the correct choice of space group for the $x = 0.75$, 1.0 and 1.25 samples is indeed monoclinic $P2_1/n$ ($\mathbf{a} = \mathbf{a}_p + \mathbf{b}_p$, $\mathbf{b} = -\mathbf{a}_p + \mathbf{b}_p$,

Table 2
Refined structural parameters for $SrCaCrNbO_6$ from room temperature X-ray powder diffraction data

Atom	x	y	z	B_{iso}	N
Ca	−0.0003(20)	0.5008(9)	0.2500(23)	2.12(2)	0.5
Sr	−0.0003(20)	0.5008(9)	0.2500(23)	2.12(2)	0.5
Cr1	0	0	0	0.80(2)	0.24(1)
Nb1	0	0	0	0.80(2)	0.26(1)
Cr2	0	0	$\frac{1}{2}$	0.80(2)	0.26(1)
Nb2	0	0	$\frac{1}{2}$	0.80(2)	0.24(1)
O1	0.1907(26)	0.2681(23)	−0.0346(17)	−0.95(4)	1.0
O2	0.2412(21)	0.7921(19)	−0.0173(16)	−0.95(4)	1.0
O3	0.0589(21)	−0.0420(20)	0.2618(22)	−0.95(4)	1.0

$a = 5.5242(4)$, $b = 5.5137(3)$, $c = 7.7978(4)$, $\beta = 90.00(4)^\circ$, $R_p = 2.17$, $R_{wp} = 3.02$.

$\mathbf{c} = 2\mathbf{c}_p$; $\mathbf{a}^* = {}^1/_2[110]_p^*$, $\mathbf{b}^* = {}^1/_2[\bar{1}10]_p^*$, $\mathbf{c}^* = {}^1/_2[001]_p^*$). Fig. 4, for example, shows (a) [010] and (b) [110] zone axis EDPs of the $x = 0.75$ sample while (c) shows an [001] zone axis EDP of the $x = 1.25$ sample and (d) a $[11\bar{2}]$ zone axis EDP of the $x = 1.0$ sample. Equivalent zone axis EDPs to these were obtained for each composition. Close inspection of some of these EDPs sometimes showed evidence for more than one orientational twin domain being simultaneously illuminated e.g. very weak $\mathbf{G} \pm 1/2\ [100]_p^*$ satellite reflections are present in Fig. 4c (compare e.g with Fig. 4b).

The fourth oxide $x = 1.5$ sample appears to be a two phase sample. Some grains show only $G \pm 1/2\ \langle 111 \rangle_p^*$ type satellite reflections (see e.g. Fig. 5a and b) and are thus only compatible with resultant $Fm\bar{3}m$ ($a = 2a_p$) or $I4/m$ ($\mathbf{a} = \mathbf{a}_p + \mathbf{b}_p$, $\mathbf{b} = -\mathbf{a}_p + \mathbf{b}_p$, $\mathbf{c} = 2\mathbf{c}_p$) space group symmetries.

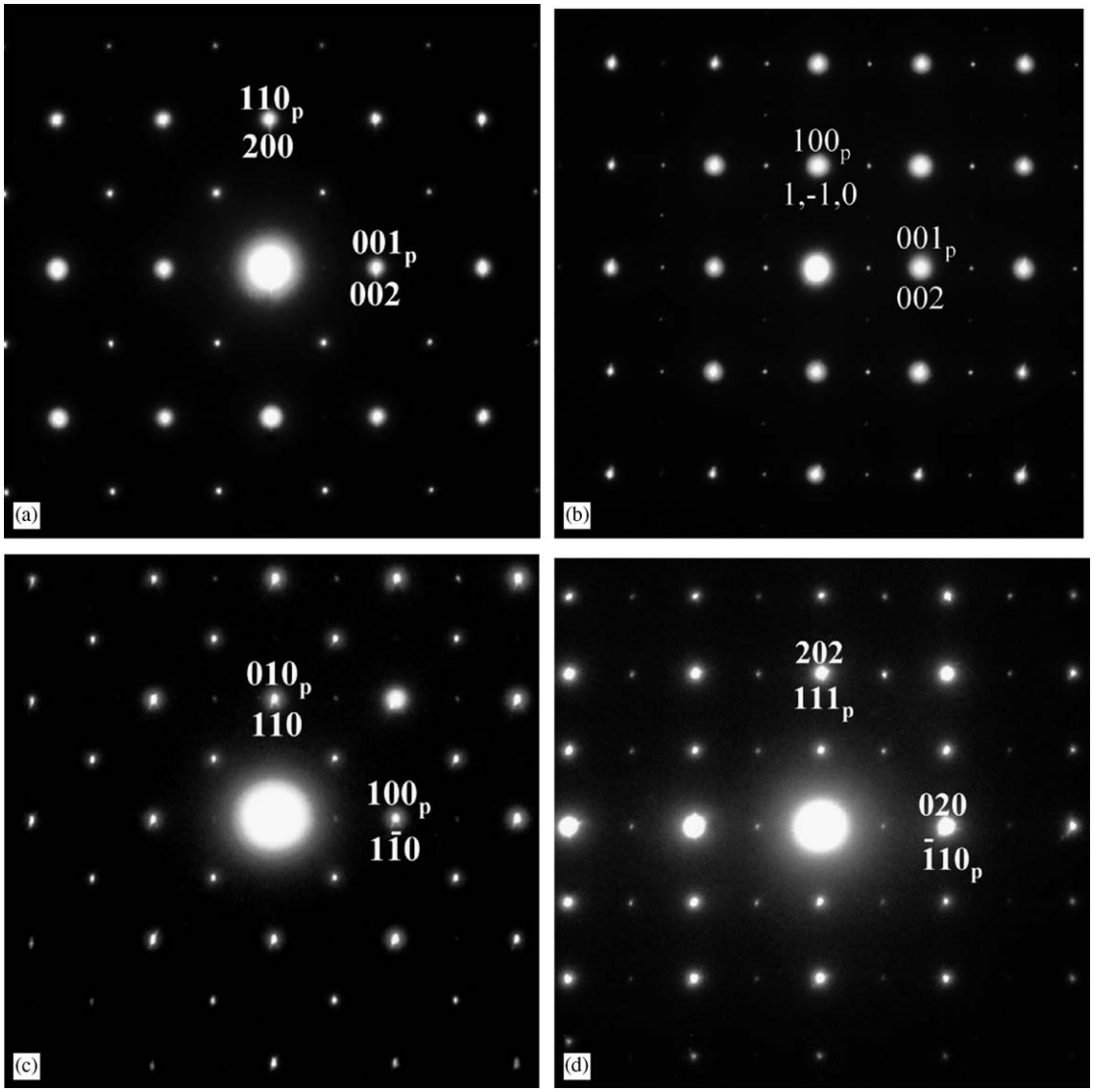

Fig. 4. Electron diffraction patterns for (a) [010] and (b) [110] zone axis of the $x = 0.75$ sample (c) a [001] zone axis of the $x = 1.25$ sample and (d) a [112] zone axis of the $x = 1.0$ sample.

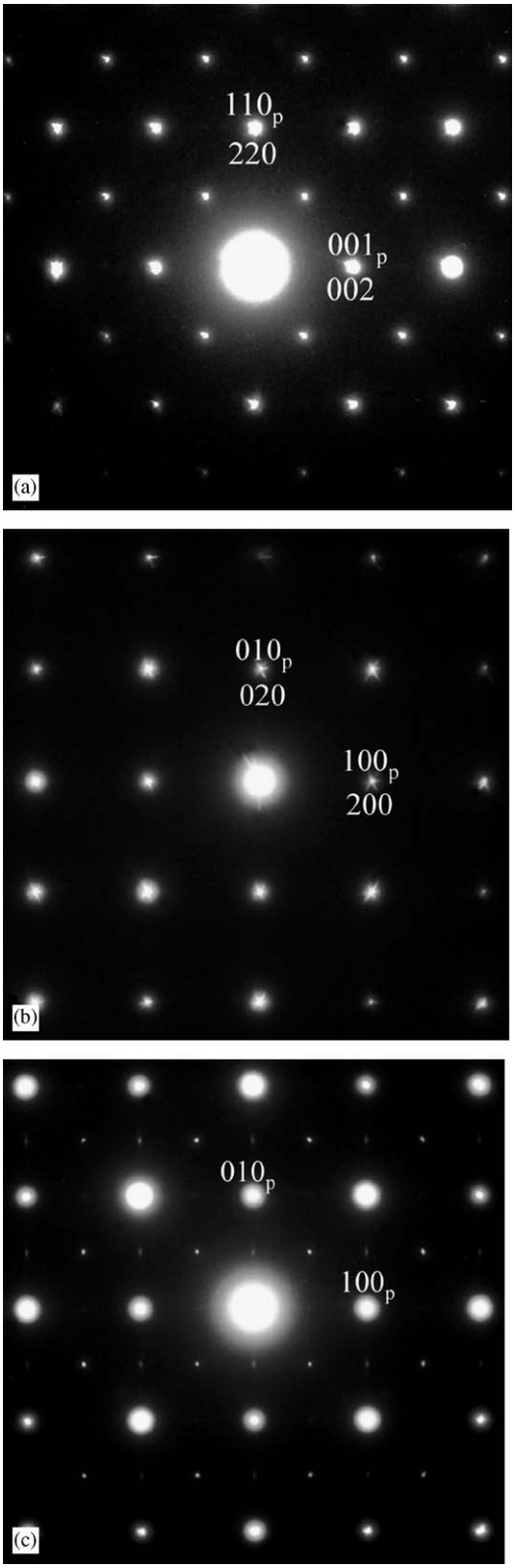

Fig. 5. Electron diffraction patterns for Sr1.5Ca0.5CrNbO6. The patterns in (a) and (b) show only $G\pm1/2\langle111\rangle$p* type satellite reflections whereas (c) shows both $G\pm1/2$ [110]p* and $G\pm1/2$ $\langle001\rangle$p* type satellite reflections.

Note that these two space group symmetries cannot be distinguished via conventional selected area electron diffraction as they both give rise to entirely equivalent zone axis EDPs. The three-fold symmetry of convergent beam EDPs, when taken down a $\langle111\rangle_p$ zone axis direction, however, strongly suggests $Fm\bar{3}m$ rather than $I4/m$ space group symmetry. Other grains from the same sample, however, show both $G\pm1/2$ $[110]_p$* and $G\pm1/2$ $\langle001\rangle_p$* type satellite reflections as well (see e.g. Fig. 5) and thus appear to be consistent with $P2_1/n$ space group symmetry. Thus the electron diffraction studies suggest that the structure transforms directly from $P2_1/n$ to $Fm\bar{3}m$.

The composition dependence of the volume for the series $Sr_{2-x}Ca_xCrNbO_6$ is illustrated in Fig. 6 and shows a progressive reduction in volume as the amount of the smaller Ca^{2+} cation is increased. There are two important features from this figure. Firstly, there is no obvious discontinuity in the volume associated with the transition from monoclinic to cubic, although there is an apparent discontinuity in the individual lattice parameters near $x = 0.75$, that is near the composition that the electron diffraction studies show the samples to be two-phase. Secondly the volume follows Vegard's law (liner relationship between composition and volume) although there is a strong variation from in the linearity of the individual lattice parameters this at high Ca contents. The introduction of the smaller Ca cation into the structure placing the structures under some stain, and this strain is associated with the monoclinic distortion.

The failure to observe any phases intermediate between the monoclinic and cubic structures is unusual and indicates that the phase transition between these must be first order. Clearly, the composition steps are, by necessity relatively course, and it is possible that an intermediate phase exists over a very small range of compositions. An alternate method of studying the transition at finer

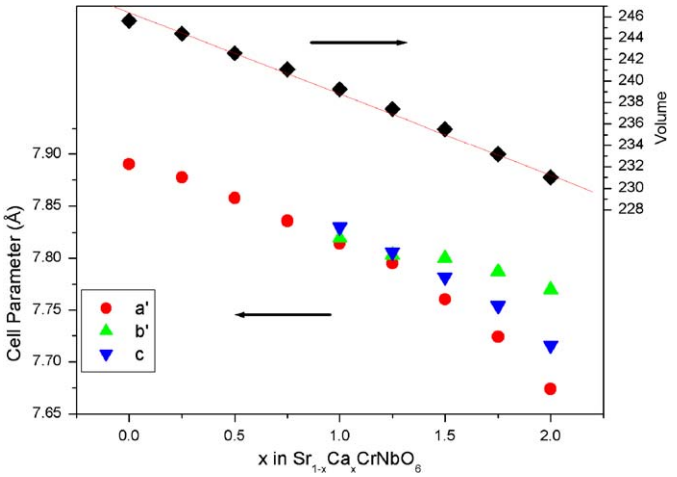

Fig. 6. Variation of the lattice parameters and volume in the series $Sr_{2-x}Ca_xCrNbO_6$. The lattice parameters in the monoclinic phase have been scaled for ease of comparison. The solid line is a linear fit to variation in volume.

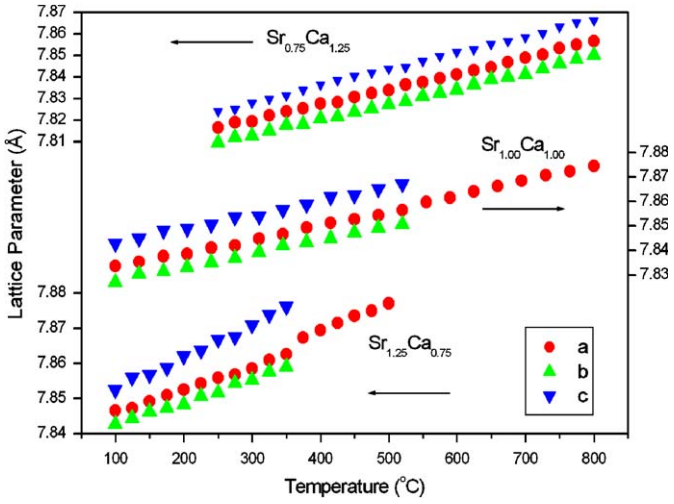

Fig. 7. Temperature dependence of the lattice parameters for selected members of the series $Sr_{2-x}Ca_xCrNbO_6$. The lattice parameters of the monoclinic phase have been scaled for ease of comparison. The transition to cubic appears to be first order and the temperature of this increases with increasing Ca content.

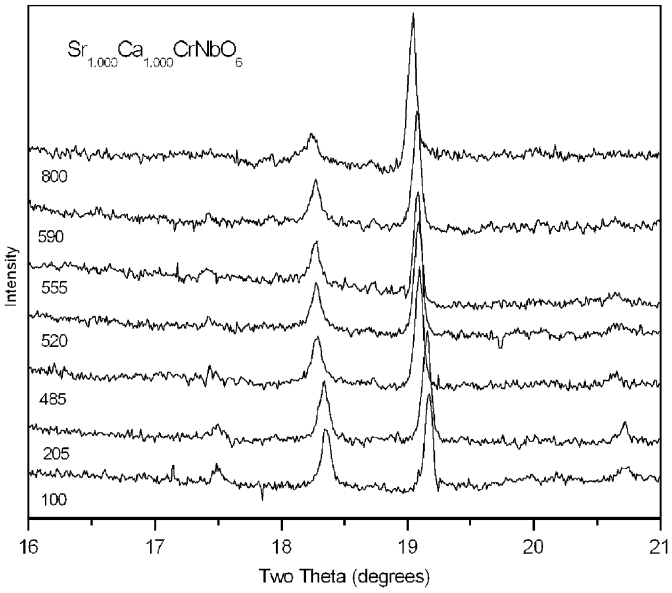

Fig. 8. Portions of the synchrotron diffraction profiles for $Sr_{1.000}Ca_{1.000}CrNbO_6$ showing the loss of weak X-point superlattice reflections near $2\theta = 17.5^\circ$ (120/210) and $2\theta = 21.7^\circ$ (212) above 590 °C.

increments is to use variable temperature data and accordingly synchrotron diffraction patterns were collected for three samples $Sr_{1.25}Cr_{0.75}CrNbO_6$, $Sr_{1.00}Cr_{1.00}CrNbO_6$ and $Sr_{0.75}Cr_{1.255}CrNbO_6$ as a function of temperature. The structures of these oxides were monoclinic at room temperature and it was anticipated that the distortion would decrease as the temperature was increased as observed for other perovskites such as $CaTiO_3$ [19] and $SrZrO_3$ [20].

The results of these studies are summarized in Fig. 7. As for the room temperature studies the space group could not be established from the cell metric (splitting of the Bragg reflections), but rather was identified by the superlattice reflections and the transition to cubic was deemed to have occurred when these could no longer be identified. A typical series of profiles is illustrated in Fig. 8. It was concluded that the transition to cubic occurred near 350 °C for $Sr_{1.25}Cr_{0.75}CrNbO_6$, and at about 525 °C in $Sr_{1.00}Cr_{1.00}CrNbO_6$. Diagnostic X-point superlattice reflections were still observed in the pattern of $Sr_{0.75}Cr_{1.255}CrNbO_6$ at 800 °C (the highest temperature available to us) showing this remains monoclinic to above this temperature. The temperature dependence of the lattice parameters show the transition to cubic is first order, as is required by group theory [16]. There is no evidence for any intermediate phase, suggesting either a direct first order $P2_1/n$ to $Fm\bar{3}m$ transition or that the intermediate phase was a very limited stability domain. It appears not to be possible to distinguish between these possibilities using X-ray diffraction.

In conclusion complete solubility is observed in the series $Sr_{2-x}Ca_xCrNbO_6$, all of which exhibit rock-salt like ordering of the Cr^{3+} and Nb^{5+} cations. The crystal structures of the end members of the series Sr_2CrNbO_6 and Ca_2CrNbO_6 are cubic in $Fm\bar{3}m$ and monoclinic in $P2_1/n$, respectively. The structures were refined using powder neutron and synchrotron X-ray powder diffraction data and the refinements demonstrate that there is considerable anti-site Cr–Nb mixing. Variable temperature and/or composition studies suggest a direct first order $P2_1/n$ to $Fm\bar{3}m$ transition a suggestion supported by selected area electron diffraction studies.

Acknowledgments

This work has been partially supported by the Australian Research Council. The work performed at the Australian National Beamline Facility was supported by the Australian Synchrotron Research Program, which is funded by the Commonwealth of Australia under the Major National Research Facilities program. The assistance of Dr. James Hester at the ANBF is gratefully acknowledged.

References

[1] R.H. Mitchell, Perovskites: Modern and Ancient, Almaz Press, Ontario, Canada, 2002.
[2] K.L. Kobayashi, T. Kimura, H. Sawada, K. Terakura, Y. Tokura, Nature 395 (1998) 677–680.
[3] B. Garcia-Landa, C. Ritter, M.R. Ibarra, J. Blasco, P.A. Algarabel, R. Mahendiran, J. Garcia, Solid State Commun. 110 (1999) 435.
[4] M.T. Anderson, K.B. Greenwood, G.A. Taylor, K.R. Poeppelmeier, Prog. Solid State Chem. 22 (1993) 197.
[5] J.H. Choy, S.T. Hong, K.S. Choi, J. Chem. Soc. Faraday Trans. 92 (1996) 1051.
[6] R.D. Shannon, Acta Crystallogr. A 32 (1976) 751.
[7] B.J. Kennedy, B.A. Hunter, J.R. Hester, Phys. Rev. B 65 (2002) 224103.
[8] B.J. Kennedy, K. Yamaura, E. Takayama-Muromachi, J. Phys. Chem. Solids 265 (2004) 1065.

[9] L. Li, B.J. Kennedy, Y. Kubota, K. Kato, R.F. Garrett, J. Mater. Chem. 14 (2004) 263–273.
[10] B.J. Kennedy, C.J. Howard, G.J. Thorogood, J.R. Hester, J. Solid State Chem. 161 (2001) 106.
[11] T.M. Sabine, B.J. Kennedy, R.F. Garrett, G.J. Foran, D.J. Cookson, J. Appl. Crystallogr. 28 (1995) 513.
[12] C.J. Howard, B.A. Hunter, A computer program for Rietveld analysis of X-ray and neutron powder diffraction patterns, Lucas Heights Research Laboratories, NSW, Australia, 1998, pp. 1–27.
[13] T. Kamiyama, S. Torii, K. Mori, K. Oikawa, S. Itoh, M. Furusaka, S. Satoh, T. Egami, F. Izumi, H. Asano, Mater. Sci. Forum 321–324 (2000) 302–307.
[14] A.C. Larson, R.B. Von Dreele, General structure analysis system (GSAS), Los Alamos National Laboratory Report LAUR 86-748, 1994.
[15] P.M. Woodward, Acta Crystallogr., Sect B: Struct. Crystallogr. Cryst. Chem. 53 (1997) 44.
[16] C.J. Howard, B.J. Kennedy, P.M. Woodward, Acta Crystallogr., Sect B: Struct. Crystallogr. Cryst. Chem. B 59 (2003) 463.
[17] Q. Zhou, B.J. Kennedy, J. Phys. Chem. Solids 2006, in press.
[18] C.J. Ball, B.D. Begg, D.J. Cookson, G.J. Thorogood, E.R. Vance, J. Solid State Chem. 139 (1998) 238.
[19] B.J. Kennedy, C.J. Howard, B.C. Chakoumakos, J. Phys. C: Condens. Matter 11 (1999) 1479.
[20] C.J. Howard, K.S. Knight, B.J. Kennedy, E.H. Kisi, J. Phys. C: Condens. Matter 12 (2000) L677–L683.